



Article

Evaporation of Promising Fire Extinguishing Agent Droplets

Alena Zhdanova ^{1,*} , Anastasia Islamova ², Roman Kurapov ³ and Roman Volkov ¹ 

¹ Research School of High-Energy Physics, National Research Tomsk Polytechnic University, 634050 Tomsk, Russia

² Heat and Mass Transfer Laboratory, National Research Tomsk Polytechnic University, 30 Lenin Ave., 634050 Tomsk, Russia

³ School of Energy and Power Engineering, National Research Tomsk Polytechnic University, 634050 Tomsk, Russia

* Correspondence: zhdanovaao@tpu.ru; Tel.: +7-(3822)-701-777 (ext. 3461)

Abstract: Woodland fires are a major issue worldwide. The aviation method of extinguishing forest fires is one of the main ones. However, the use of the latter is carried out according to the results of experiments, bench or flight tests in the absence of models that adequately describe the mechanisms for suppressing the combustion of forest combustible materials with specific fire extinguishing compositions (solutions, emulsions or suspensions). Therefore, the task of studying the evaporation and interaction of single drops with the surfaces of combustible materials is relevant and practically significant in the field of fire hazards. The paper presents the experimental research findings on the evaporation of specialized composition droplets for extinguishing fires under different heat supply schemes. The compositions under study included a group of widely used fire extinguishing agents: water; flame retardant FR-Les (5% solution); FR-Les (20% solution); bentonite slurry (1%); bentonite slurry (5%); bischofite solution (5%); bischofite solution (10%); fire extinguishing agent OS-5 (5% solution); fire extinguishing agent OS-5 (10% solution); fire extinguishing agent OS-5 (15% solution); foaming agent emulsion (1%); foaming agent emulsion (5%); fire retardant (5% solution). Specialized composition droplets were heated using conductive, convective and radiant heating. Empirical coefficients were obtained.

Keywords: fire extinguishing agents; droplets; high-temperature heating; different heating schemes; evaporation



Citation: Zhdanova, A.; Islamova, A.; Kurapov, R.; Volkov, R. Evaporation of Promising Fire Extinguishing Agent Droplets. *Forests* **2023**, *14*, 301. <https://doi.org/10.3390/f14020301>

Academic Editor: Costantino Sirca

Received: 29 December 2022

Revised: 1 February 2023

Accepted: 2 February 2023

Published: 3 February 2023



Copyright: © 2023 by the authors. Licensee MDPI, Basel, Switzerland. This article is an open access article distributed under the terms and conditions of the Creative Commons Attribution (CC BY) license (<https://creativecommons.org/licenses/by/4.0/>).

1. Introduction

Controlling the drying process of colloidal solutions is of interest for diagnostic method development [1], microchip production [2] and fire suppression [3]. Findings have been reported on the way the solution concentration [4], ambient conditions (e.g., temperature [5] and moisture content [6,7]) and surface types [8] affect the evaporation regimes and rates, as well as on the geometrical characteristics of droplets during their evaporation. The majority of experimental studies involve model colloidal particles with known physical and chemical properties (e.g., polymer [9,10] and silica [9,11] micro- and nanoparticles). The evaporation of these solutions occurs with a gradual accumulation of colloids at the air-liquid interface throughout the whole process. The evaporation of droplets containing nonvolatile materials leaves a deposit or “film” [12]. The shape and appearance of the solid deposit are correlated with the internal stress of the flow (caused by evaporation) and with the mechanical properties of the materials involved. The formation of the film (or the skin) is essentially due to the competition between evaporation and diffusive Brownian motion [13]. Therefore, droplet evaporation is attracting an increasing interest of researchers in the fields of soft condensed matter and fluid mechanics. In the evaporation of a saline solution droplet, the solvent evaporation leads to the saturation of the solute, resulting in its crystallization. An increase in the salt concentration increases the surface tension. An increase in the concentration of colloids or polymers reduces the liquid surface tension.

Significantly, the evaporation mechanisms of pendant and sessile droplets are different. Hampton et al. [14] explored the effect of the surface orientation on the solid deposit. Unlike sessile water droplets containing nanoparticles of silicon dioxide, leaving a “coffee ring” upon evaporation [15], a pendant droplet forms a small and dense deposit of particles in the center of the drop [14]. Li et al. [16] investigated the role of gravity in particle sorting during the evaporation of a suspended droplet. Due to the lack of foundation support and the weaker influence of the surface tension, the morphology of the deposit depends greatly on the gravity forces. The dependence of the diameter and temperature of droplets on time during their evaporation in a hot air flow was obtained (velocity up to 3.1 m/s, temperature 150 °C) [17]. The evaporation of a droplet at a higher gas temperature (up to ~1000 K) was performed in [18,19]. The influence of the suspender material on the droplet evaporation was considered in [20,21]. An increase in the suspender thickness was found [20] to increase the thermal conductivity between the suspender and the droplet. The heating from the support fiber can generate strong capillary flows on the droplet surface [20]. Yet Shih et al. [21] showed that the effect of conductivity on the material was insignificant in environments with forced convection and at high temperatures.

In terms of fire suppression, the wettability and coating properties of the following specialized fire extinguishing agents were considered: saline solutions ($K_3[Fe(CN)_6]$ [22], $CuCl_2$ [23]), foaming agent emulsions (W-50, W-52, W-56, W-10, W-11 and W-32 [24]; non-ionic and anionic surfactants [25]; L-77 [26]), clays [27], different types of fire retardants (Borax ($Na_2B_4O_7$), DSHP (Na_2HPO_4), DAHP ($(NH_2)_4HPO_4$) and DW [28]), etc. Although some research has been carried out on the behavior of composition droplets during their evaporation, there is still very little scientific understanding of their fire-retardant mechanisms. Boreal forest fires [29,30] are often combated using aerial firefighting [31,32]. Notably, when arrays of fire extinguishing agents travel the distance from the plane board to a thermally decomposing material, they deform and break up into smaller agglomerates. These patterns of fire-extinguishing agent array destruction and transformation are described in detail in [33]. At the same time, the evaporation of specialized composition droplets covering the distance from the dropping location on the aircraft board to a thermally decomposing forest fuel differs significantly due to different heating mechanisms [34].

Effective fighting against forest fires is inextricably linked with the use of special fire extinguishing compositions. Drops of liquid and special compounds are the main tools for temperature control when interacting with combustible forest material. The surfaces of elements of forest combustible materials are characterized by a chaotic arrangement of inhomogeneities, which affect the processes of wetting, spreading and evaporation of fire extinguishing agents, and hence the effectiveness of fire extinguishing. Moreover, not only when extinguishing forests, but also when localizing the burning of equipment, various buildings and structures. The purpose of this research is to determine the characteristics of evaporation of promising fire extinguishing agent droplets when varying the temperature and heat supply method.

2. Materials and Methods

2.1. Materials

The compositions under study were distilled water and specialized water-based compositions with typical fire extinguishing agents added to them. The images of additives to water and compositions are presented in Figure 1. The physical properties and chemical composition of some of the mixtures are summed up in Table 1. The concentrations in the compositions were chosen following the guidelines from [35–38].

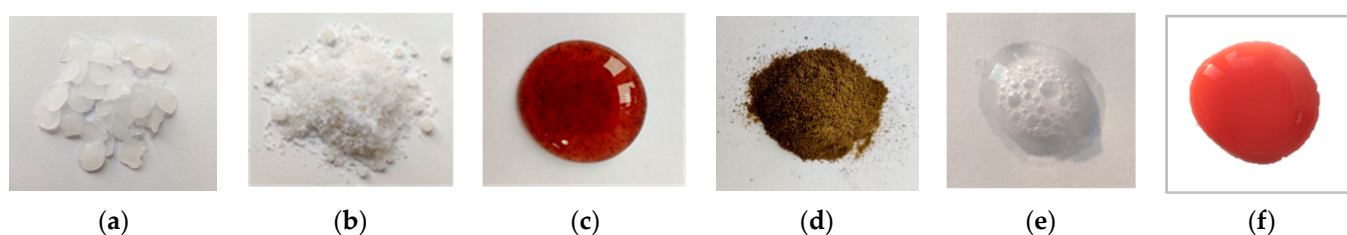


Figure 1. Images of additives to water and fire extinguishing agents: (a) bischofite; (b) OS-5; (c) FR-Les solution; (d) bentonite; (e) foaming agent emulsion; (f) fire retardant solution.

Table 1. Characteristics of fire extinguishing agents and water at $T_{cp} = 20\text{ }^{\circ}\text{C}$ [35–38].

Firefighting Compositions	Bischofite Solution	OS-5 Solution	FR-Les Solution	Bentonite Slurry	Foaming Agent Emulsion	Water	
$C, \%$	10	10	5	20	5	-	
$\gamma, \text{mN/m}$	75.8	45	37.26	35.02	68.5	17.3	
$\rho, \text{kg/m}^3$	1081.5	1099.1	1019	1047	1100	1002–1187	
$\lambda_m, \text{W/(m}\cdot\text{K)}$	0.58	0.624	0.704	0.704	0.5952	0.599	
$\mu \cdot 10^3, \text{Pa}\cdot\text{s}$	1.015	0.12	3.02	3.65	24.3	0.12	
Chemical composition (information from public sources)	$\text{MgCl}_2 \cdot 6\text{H}_2\text{O}$ (93%); the rest are impurities	Carbamide (31%–32%); alkylbenzene sulfonate (2%–3%); acid dye (0.5%–1%); ammonium chloride (13%–15%); diammonium phosphate (the rest)	Ammonium polyphosphate solution, phosphorus pentoxide (31.5%); nitrogen (9%)	Montmorillonite $\text{Si}_8\text{Al}_4\text{O}_{20}(\text{OH})_4 \times n\text{H}_2\text{O}$ (60%–70%); the rest are sandy-aleuritic material impurities	Silicon dioxide (60%–65%); aluminum oxide and iron oxide (20%–25%)	Fluoridated surfactants	Binary inorganic compound whose molecule consists of two hydrogen atoms and one oxygen atom (the atoms are linked by covalent bonds)

2.2. Evaporation of Fire Extinguishing Agent Droplets

Four heating schemes were employed to investigate the evaporation of fire extinguishing agent droplets: conduction (using a PLK-1818 hot plate), convection (in a gas flow) and radiation (in a muffle furnace and over an open flame). Each of these schemes corresponds to the conditions of real fires: when droplets pass through a combustible gas front (convective and radiant heating) and a flame ends up on a heated combustible material (conductive heating). Typical images obtained in the experiments are shown in Figure 2.

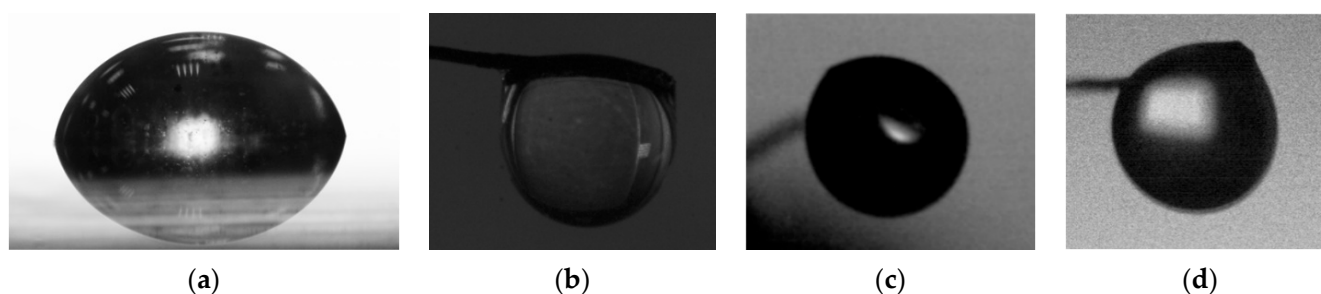


Figure 2. Typical images of water droplets using conductive (a), convective (b), radiant heating in a muffle furnace (c) and a view above the burner (d).

2.2.1. Evaporation of Fire Extinguishing Agent Droplets Using Conductive Heating

To identify the main patterns of evaporation of specialized fire extinguishing agent droplets, the experimental setup shown schematically in Figure 3 was employed. The method used in the research was shadowgraphy.

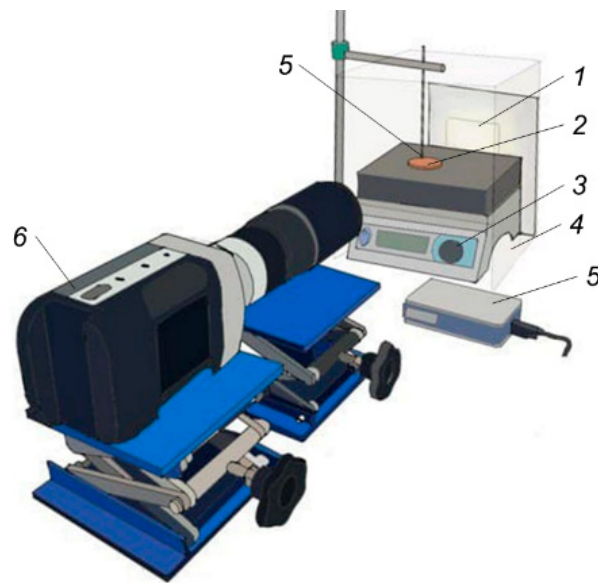


Figure 3. Experimental setup: (1) light source; (2) investigated surface; (3) PLK-1818 hot plate; (4) box; (5) thermocouple; (6) high-speed camera.

In the experiments involving heating, a polished steel substrate ASTM A 240/A 240M 430 (Fe 82.701, C 0.046, Si 0.38, Mn 0.36, P 0.029, S 0.003, Ni 0.22, Cr 16.23 and N 0.031 in wt%) 2 was fitted to a copper substrate surface with a bolted connection using thermal interface material. A polished steel surface was chosen for its low thermal conductivity and inertia, along with its minimum roughness (to counteract the effect of texture characteristics on the wettability and evaporation characteristics). A Micro Measure 3D station profilometer was used to estimate the surface roughness. The root mean square roughness (S_q) of steel was $0.06 \mu\text{m}$, the maximum height of the surface (S_z) was $0.11 \mu\text{m}$.

Two chromel-alumel thermocouples (type K) were placed between the surfaces. The substrates, fastened together, were placed on the hot plate 3 (PLK-1818). The metal surface temperature was the main variable factor in the study of the wetting properties of different liquids. The temperature on the metal surface was measured with the thermocouple 5, which was fixed perpendicularly to the surface. The surface temperature was varied in the range between 20 and $160 \text{ }^\circ\text{C}$ with an increment of $20 \text{ }^\circ\text{C}$.

A droplet of the composition under study was generated at a random point using a dispenser. Shadowgraphs of droplets were obtained using the light source 1 and the high-speed video camera 6. The droplet volume in the experiments on wetting was constant at $10 \mu\text{L}$. The contact radii of droplets with a volume of $10 \mu\text{L}$ did not exceed the capillary constant (L) of the compositions under study. Under these conditions ($r \leq L = \gamma/(\rho \cdot g)$), the size of the droplet determining the gravity acting on it had no effect on the static contact angle. The geometric characteristics of droplets (contact angle (θ), diameter (d) and height (h)) were determined at the initial moment of their interaction with the steel surface using the method from [39].

The setup was isolated from the possible influence of external, uncontrolled factors (fluctuations of temperature and air velocity in the laboratory) with a transparent box made of 3-mm-thick polymer glass. It provided constant heat exchange with the external environment. The geometric characteristics of droplets were measured at least three times.

2.2.2. Evaporation of Fire Extinguishing Agent Droplets during Convective Heating

A schematic image of the setup used to study the main evaporation characteristics during convective heating is shown in Figure 4.

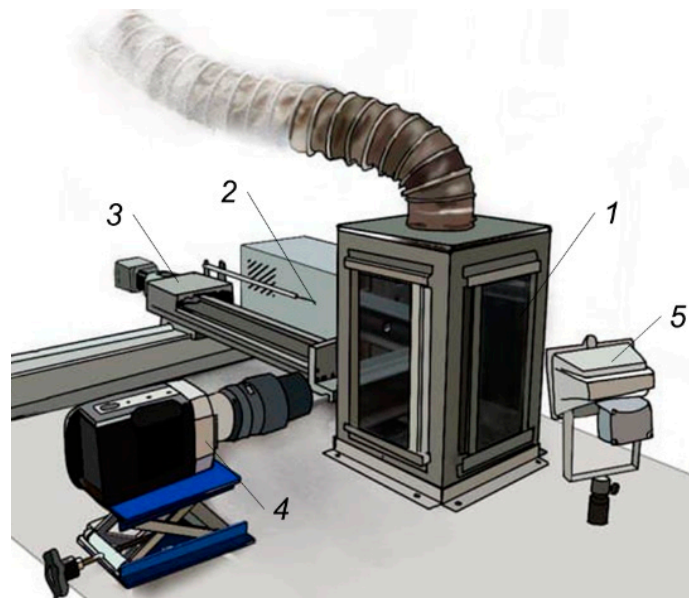


Figure 4. Experimental setup: (1) convective channel; (2) holder; (3) positioning mechanism; (4) high-speed video camera; (5) light source.

A flow of heated air in channel 1 was formed using a compressor and a heater. A 10- μ L droplet of a fire extinguishing agent was generated on the holder made of nichrome wire (0.2 mm in thickness) 2. After that, the positioning mechanism 3 placed the droplet into the heated air flow through an inlet in the cylinder wall. The high-speed video camera 4 captured the images of the droplet evaporation. The liquid droplet heating temperature was varied in the range of 100–500 °C with an increment of 100 °C. The air flow velocity was constant at 3 m/s.

2.2.3. Evaporation of Fire Extinguishing Agent Droplets during Radiant Heating

Figure 5 schematically shows the setup used to determine the key patterns of fire extinguishing agent droplet evaporation when using radiant heating.

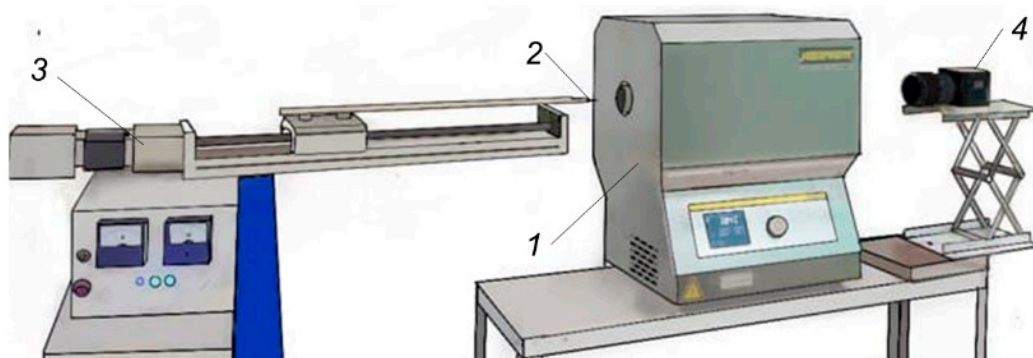


Figure 5. Experimental setup: (1) muffle furnace; (2) holder; (3) positioning mechanism; (4) high-speed video camera.

The muffle furnace 1 was heated to a specified temperature. It varied in a wide range from 100 to 1000 °C. A liquid droplet suspended on the holder (nichrome wire) 2 was placed into the furnace using the positioning mechanism 3. A Phantom V411 video camera 4 with HD 720i (1280 × 720 pixels) recorded the evaporation process at a frame rate of 100 fps.

2.2.4. Evaporation of Fire Extinguishing Agent Droplets during Open Flame Heating

Experiments in which an open flame was used to heat droplets to study their evaporation were also carried out. The burner 1 was used for that (Figure 6). Denatured alcohol was used as a fuel.

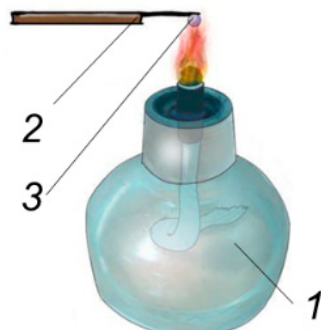


Figure 6. Schematic image of the experimental setup: (1) burner; (2) holder; (3) fire extinguishing agent droplet.

A 10- μL droplet of a fire extinguishing agent was suspended on the holder made of nichrome wire 2. The positioning mechanism placed the droplet in the recording area. A Phantom V411 video camera with HD 720i (1280 \times 720 pixels) recorded the evaporation process at a frame rate of 100 fps. A spotlight illuminated the droplet. The temperature in the experiments was varied by changing the height of the droplet placement above the burner wick (1 cm, 2 cm, 3 cm and 4 cm). A fast-response thermocouple and a National Instruments data collection module were used to measure the burner flame temperature [1]. The maximum flame temperature was ~ 850 $^{\circ}\text{C}$ at a distance of 2 cm above the wick.

3. Results

3.1. Heated Steel Surface Wetting by Fire Extinguishing Agents during Conductive Heating

Table 2 shows the static contact angles, diameter and height of liquid droplets at different temperatures of the polished steel surface. The contact angles of distilled water droplets were found to decrease by 10.4° (from 87.4° to 77°) with an increase in the surface temperature. With a temperature increase from 0 to 100 $^{\circ}\text{C}$, the surface tension coefficient of water decreases by about a quarter. This improves the wetting properties. When a fire retardant, FR-Les, bentonite and bischofite with a concentration of 5% were added, there were no significant changes in the wetting properties. The physical properties (surface tension, viscosity) of the liquids based on their composition are similar to those of water. When the compositions FR-Les (5% and 20%) and bischofite (5% and 10%) interact with combustible materials heated to high temperatures, they are charred without flammable gas emission. Notably, the FR-Les additive contains phosphorus, which initiates the formation of coal or inorganic residue in the condensed phase [38,39]. An increase in the FR-Les solution concentration to 20% thickens it, increases its density and surface tension, while reducing its wettability. Adding bischofite to water accelerates the formation of a protective coke layer.

Table 2. Geometric characteristics of droplets (contact angles, diameters and heights) at different temperatures of a polished steel surface *.

$T, ^{\circ}\text{C}$	1	2	3	4	5	6	7	8	9	10	11	12
	$\theta, ^{\circ}$											
20	87.4	76.4	102.1	94.5	82.7	84.2	84.5	52.8	42.0	42.0	52.5	34.3
40	76.4	76.4	103.5	87.2	74.4	77.8	87.0	51.4	45.1	40.9	46.1	34.5

Table 2. Cont.

$T, ^\circ\text{C}$	1	2	3	4	5	6	7	8	9	10	11	12
60	85.9	81.4	103.9	81.8	94.2	90.6	74.6	44.7	38.7	40.6	44.1	33.3
80	78.0	71.5	105.5	80.5	98.5	76.1	74.0	42.6	34.2	37.9	42.6	34.1
100	77.0	75.5	103.8	78.4	112.7	78.8	83.4	45.5	36.6	36.9	41.1	35.7
d, mm												
20	3.61	3.92	3.14	3.33	3.67	3.61	3.60	4.79	5.18	5.19	4.95	5.65
40	3.87	3.90	3.10	3.55	3.89	3.83	3.55	4.80	5.12	5.31	5.05	5.64
60	3.53	3.66	3.14	3.72	3.29	3.46	3.94	5.13	5.62	5.70	5.19	5.70
80	3.53	3.66	3.15	3.72	3.29	3.89	3.94	5.31	5.57	5.38	5.19	5.70
100	3.85	3.90	3.09	3.79	2.74	3.80	3.65	4.85	5.24	5.45	5.25	5.62
h, mm												
20	1.53	1.36	1.74	1.66	1.50	1.53	1.54	0.98	0.89	0.87	0.96	0.75
40	1.40	1.38	1.78	1.56	1.42	1.41	1.56	1.00	0.88	0.83	0.94	0.75
60	1.57	1.49	1.74	1.47	1.70	1.60	1.37	0.88	0.76	0.75	0.86	0.73
80	1.57	1.49	1.71	1.47	1.70	1.38	1.37	0.82	0.78	0.80	0.86	0.73
100	1.41	1.38	1.78	1.44	1.96	1.43	1.51	0.97	0.85	0.80	0.84	0.74

* 1—water; 2—flame retardant FR-Les (5% solution); 3—FR-Les (20% solution); 4—bentonite slurry (1%); 5—bentonite slurry (5%); 6—bischofite solution (5%); 7—bischofite solution (10%); 8—fire extinguishing agent OS-5 (5% solution); 9—OS-5 (10% solution); 10—OS-5 (15% solution); 11—foaming agent emulsion (1%); 12—foaming agent emulsion (5%).

Some patterns emerged from the analysis of Table 2. In particular, with an increase in the steel surface temperature from 20 to 100 °C, the wettability of the bentonite slurry (1%) and of water (Table 2) improves. However, with an increase in the bentonite slurry concentration to 5%, the static contact angle increases from 82.7° to 112.7° at a surface temperature of 20 and 100 °C, respectively. With a higher concentration of bentonite or FR-Les in the slurry, it becomes thick. Its properties are close to those of non-Newtonian fluids (long-term storage makes the composition thick, yet after mixing, it returns to its original state).

When the fire extinguishing agent OS-5 or the foaming agent emulsion is added to water, wettability improves because these solutions contain surfactants. The influence of surfactants on wettability is correlated with their adsorption at the phase boundary [40–42]. According to present-day ideas, the contact angle is mainly affected by the changes in the surface tension in a rather narrow region in the immediate vicinity of the three-phase contact line [41]. Surfactants reduce the liquid surface tension, thus leading to better wettability. A temperature increase reduces the liquid surface tension, contributing to the droplet spreading. The surface wettability improves with an increase in the OS-5 solution concentration from 5% to 10%. For instance, at a surface temperature of 50 °C, the contact angle decreases from 52.8° to 42.0°. However, increasing the concentration from 10% to 15% does not change the wetting properties (the contact angles are within the confidence interval). The findings suggest that OS-5 solutions with a concentration of over 10% do not change the surface tension. An assumption was made that this composition, with a concentration of over 10%, would not significantly change the thermal decomposition time of a combustible material.

Table 2 shows that an increase in the foaming agent concentration from 1% to 5% under normal conditions reduces the contact angles by more than 18°. When the substrate is heated, the difference in the angles decreases and is approx. 5° at 100 °C. It is possible to assume that with a temperature increase, the difference in the surface tension of 1% and 5% emulsions decreases. Thus, the difference in wettability becomes less substantial (i.e., when this composition is used to suppress a fire, increasing its concentration from 1% to 5% does not lead to qualitative or quantitative changes).

3.2. Evaporation of Fire Extinguishing Agent Droplets

Figures 7–10 show the times of complete evaporation of specialized fire extinguishing agent droplets as a function of the steel substrate surface temperature during conductive heating and as a function of the air temperature during convective, radiant heating and heating over the open flame of the burner.

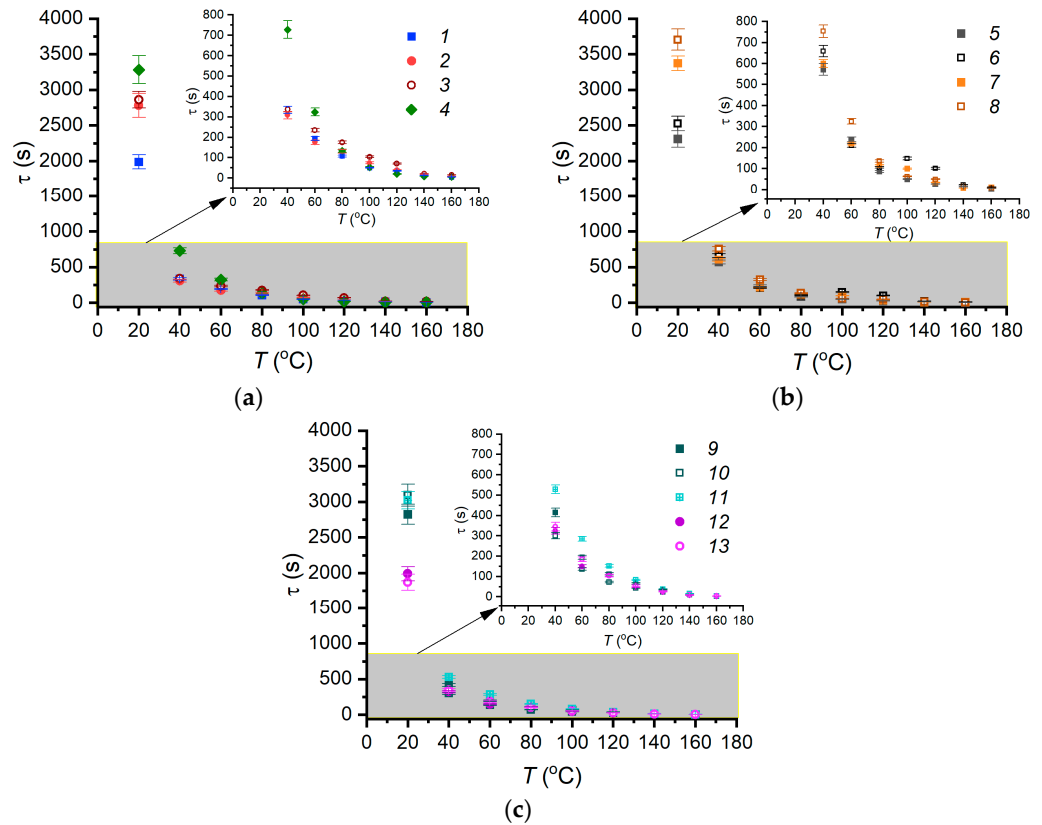


Figure 7. Evaporation time of 10- μ L droplets of fire extinguishing agents and water when varying the polished steel surface temperature: (a) 1—water; 2—flame retardant FR-Les (5% solution); 3—FR-Les (20% solution); 4—fire retardant (5% solution); (b) 5—bentonite slurry (1%); 6—bentonite slurry (5%); 7—bischofite solution (5%); 8—bischofite solution (10%); (c) 9—fire extinguishing agent OS-5 (5% solution); 10—OS-5 (10% solution); 11—OS-5 (15% solution); 12—foaming agent emulsion (1%); 13—foaming agent emulsion (5%).

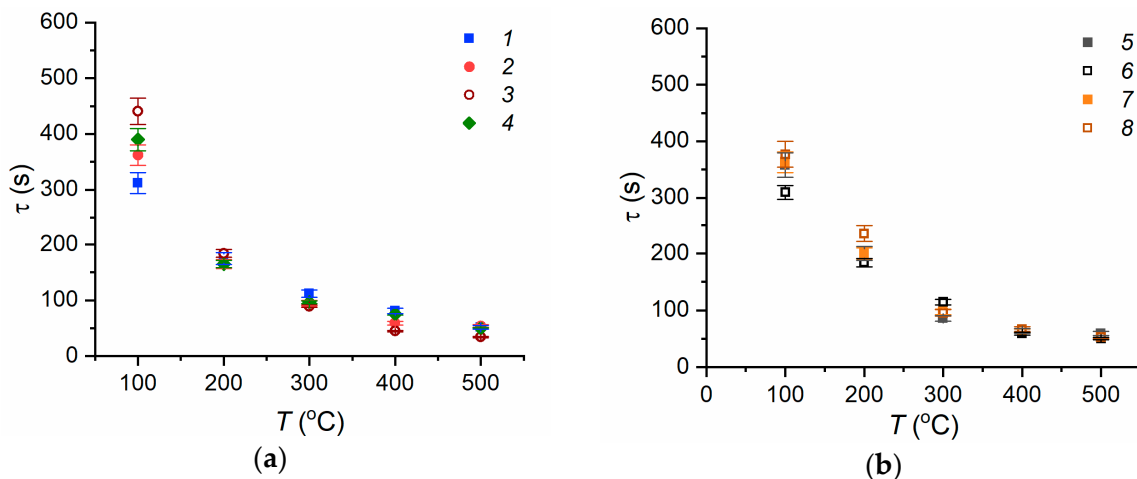


Figure 8. Cont.

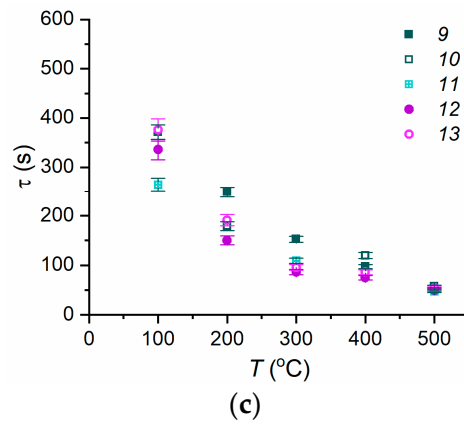


Figure 8. Evaporation time of 10- μ L droplets of fire extinguishing agents and water when varying the air temperature in the convective tube: (a) 1—water; 2—flame retardant FR-Les (5% solution); 3—FR-Les (20% solution); 4—fire retardant (5% solution); (b) 5—bentonite slurry (1%); 6—bentonite slurry (5%); 7—bischofite solution (5%); 8—bischofite solution (10%); (c) 9—fire extinguishing agent OS-5 (5% solution); 10—OS-5 (10% solution); 11—OS-5 (15% solution); 12—foaming agent emulsion (1%); 13—foaming agent emulsion (5%).

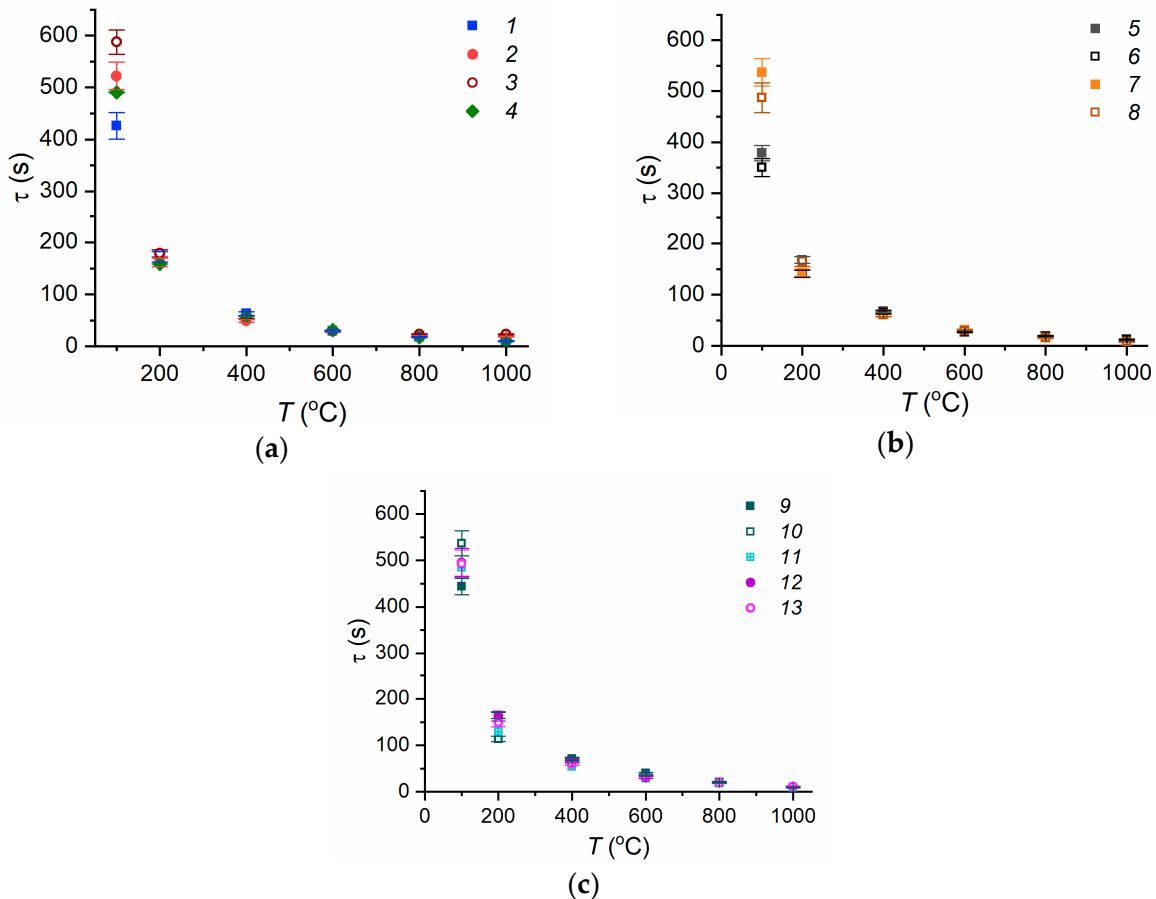


Figure 9. Evaporation time of 10- μ L droplets of fire extinguishing agents and water when varying the air temperature in the muffle furnace: (a) 1—water; 2—flame retardant FR-Les (5% solution); 3—FR-Les (20% solution); 4—fire retardant (5% solution); (b) 5—bentonite slurry (1%); 6—bentonite slurry (5%); 7—bischofite solution (5%); 8—bischofite solution (10%); (c) 9—fire extinguishing agent OS-5 (5% solution); 10—OS-5 (10% solution); 11—OS-5 (15% solution); 12—foaming agent emulsion (1%); 13—foaming agent emulsion (5%).

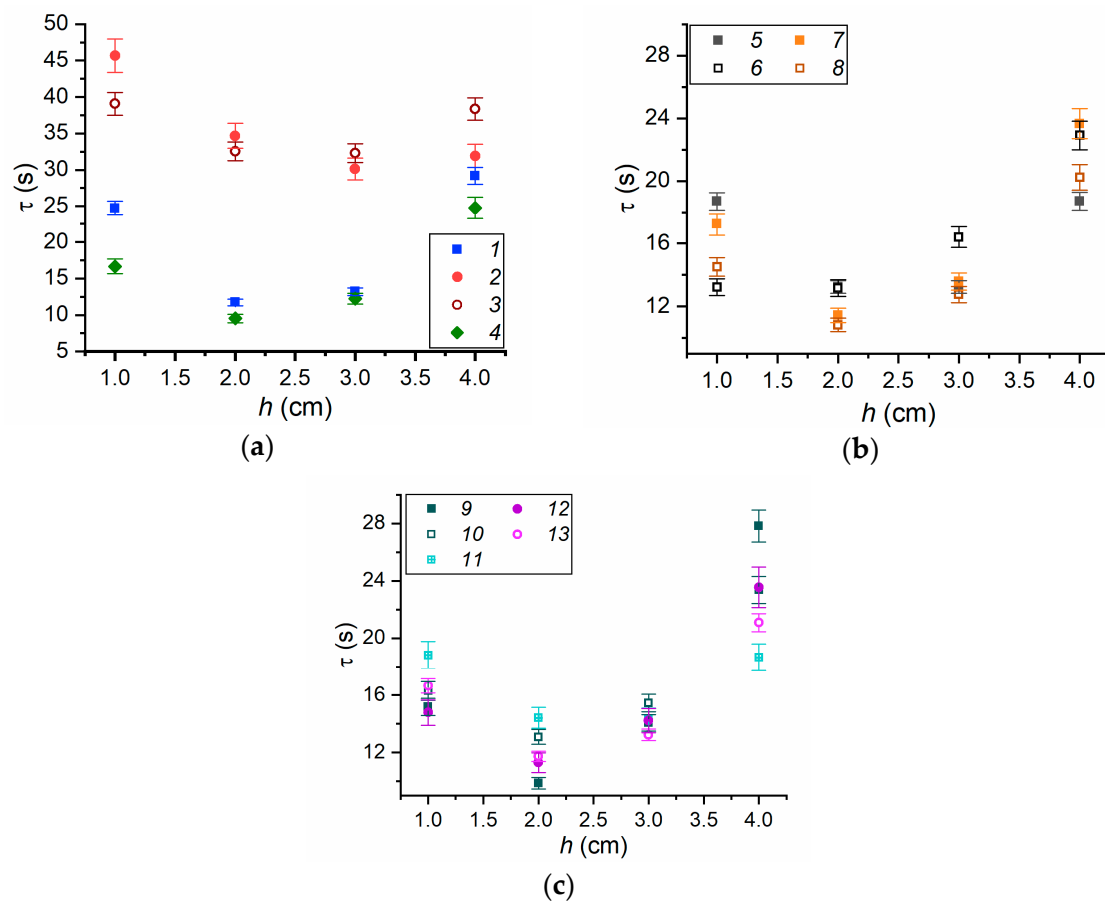


Figure 10. Evaporation time of 10- μ L droplets of fire extinguishing agents and water when varying the height of the droplet position above the open burner flame: (a) 1—water; 2—flame retardant FR-Les (5% solution); 3—FR-Les (20% solution); 4—fire retardant (5% solution); (b) 5—bentonite slurry (1%); 6—bentonite slurry (5%); 7—bischofite solution (5%); 8—bischofite solution (10%); (c) 9—fire extinguishing agent OS-5 (5% solution); 10—OS-5 (10% solution); 11—OS-5 (15% solution); 12—foaming agent emulsion (1%); 13—foaming agent emulsion (5%).

Under normal conditions of droplet evaporation on the substrate, the minimum evaporation time was recorded for the 5% foaming agent emulsion (Figure 7). This is conditioned by the fact that the liquid evaporation rate is directly proportional to the surface area (the larger the area of the liquid–air interface, the more molecules of liquid evaporate). The minimum contact angle and the maximum area were recorded for the foaming agent emulsion ($\theta \approx 35.7^\circ$, $S \approx 26.9 \text{ mm}^2$). The difference in the evaporation time of the emulsions with different concentrations was found to decrease with a higher temperature, since wettability is almost identical (Table 2). That means that this liquid is more efficient in the cooling of a combustible material than the other compositions under study. The analysis of the conducted experiments revealed that an increase in the OS-5 solution concentration from 5% to 10% reduced the evaporation time by more than 30%. A further increase in the concentration (to 15%) did not only reduce the droplet lifetime but also cut down the evaporation time by almost 2.1 times (at $T > 60^\circ \text{C}$). This leads to the conclusion that using a foaming agent and OS-5 with a concentration of more than 10% for extinguishing fires will not significantly improve the suppression of combustible material pyrolysis or combustion.

A comparative analysis shows that the evaporation times of droplets of water, 5% fire retardant, FR-Les and bischofite solutions, as well as 1% bentonite slurry, differ only slightly (Figure 7). This finding is explained by the fact that the numerical values of the thermophysical properties of these liquids (density, heat capacity) and contact angles (thus,

the droplet interaction area and the liquid–air interface) are very similar. With an increase in the concentration of FR-Les and bischofite, the evaporation times increase while the evaporation rates decrease. The evaporation of liquids based on water and fire extinguishing agents (bentonite, bischofite, FR-Les and OS-5) leaves a solid residue (bentonite, salt crystals of MgCl_2 , ammonium polyphosphate and diammonium phosphate–carbamide). Complete evaporation of water from the saline solution produces fine crystals that cover the area of the liquid-heated substrate contact. Water evaporation reduces the viscoelastic properties of the solution. As a result, the droplet spreads more. The adhesion of the liquid to the crystal ring decreases, and the liquid separates early from the original interface of three phases and slips off into the droplet. Further evaporation of the remaining water produces large salt crystals on a small area within the original droplet boundaries. This residue locks the gaseous thermal decomposition products in the pyrolysis zone because a condensed substance layer forms on the upper boundary of this zone.

In the experiments with slurries, emulsions and solutions, less heat is absorbed in the evaporation of a unit of mass of these liquids than in the evaporation of water. In the same way, more energy is spent on heat accumulation before water evaporation than it is in the case of solutions, emulsions and slurries. This conclusion is confirmed, e.g., by the analysis of the heat balance in the evaporation of water (~340 kJ) and 10% bischofite solution (~290 kJ). However, earlier findings [22,23] indicate that of all the compositions under study, water is least effective in the extinguishment of forest fuel fires. Large volumes of liquid and/or long suppression times are required. This leads to the conclusion that the dominant mechanism in the extinguishing of combustible materials and pyrolysis suppression using compositions such as fire retardants, bischofite, bentonite and FR-Les will be the formation of a protective layer on the material elements rather than the absorption of heat in the solvent evaporation. In the experiments with convective heating, thermogravitational and thermocapillary convection play a great role. It was established [2] that convection rates in the droplet increase severalfold due to thermal heating, oncoming gas flow and the geometric shape of the sample. Convection intensification in the droplet leads to the mixing of the layers. The liquid heats more rapidly, which leads to a lower surface tension of the liquid and increases the free evaporation area. This intensifies evaporation. The comparison of the evaporation times of specialized fire extinguishing agents under different heat supply conditions shows that in the radiant (in the muffle and above the burner) and convective heating of droplets (Figures 8–10), the longest evaporation time and the highest evaporation rate were typical of the 20% and 5% FR-Les solutions. Ammonium polyphosphate, being a component in the FR-Les composition, decomposes and emits a noncombustible gas when it is subjected to a high temperature. Thus, it forms a protective layer and limits oxygen access. The remaining polyphosphate acid acts as a catalyst in the foam-forming reaction when free carbon is separated from the material. This effect is especially distinct when heating the droplet over the burner. Figure S1a shows the images of a 20% FR-Les solution droplet heated over an open flame. During combustion, the emerging carbonaceous film blisters without melting (Figure S1a, $\tau \approx 6$ s) and forms a thick foam layer, thus providing heat insulation.

In convective heating, the lowest evaporation time was recorded for the 10% OS-5 solution. Low surface tension causes the droplet to spread over the holder (which means a larger free area of interaction with the heated air and thus a higher evaporation rate). For two-thirds of the evaporation time, it is only the solvent (water) that evaporates. This is followed by active foam formation with the evaporation of the remaining water and the formation of a saline film on the holder surface. Typical evaporation images are presented in Figure S1b (Supplementary Material).

The droplet evaporation rate was found to rise with an increase in the absorption indicator. During radiant heating, the amount of heat supplied to the droplet is given by:

$$\lambda \frac{\partial T}{\partial R} \Big|_{R=R_d} = \rho L \frac{dR_d}{d\tau} + \alpha(T_g - T_s) + \varepsilon c_0 T_g^4 \quad (1)$$

where λ is thermal conductivity, W/m·K; ρ is density, kg/m³; L is the latent heat of evaporation, kJ/kg; $\frac{dR_d}{d\tau}$ is the rate of the droplet radius change due to evaporation, m/s; α is heat transfer coefficient, W/m²·K; T_g is the ambient temperature, K; T_s is the droplet temperature, K; ε is emissivity factor; c_0 is the black body emissivity factor, W/(m²·K⁴). When the heating is performed in a muffle furnace and over an open flame, the $\varepsilon c_0 T_g^4$ part of the equation will make a major contribution and have a considerable effect on the droplet emissivity factor. The higher the emissivity factor, the faster the droplet evaporates. The findings obtained in this work are consistent with this statement. The lowest evaporation time was recorded for the 5% bentonite slurry, as the liquid is optically nontransparent and has the highest emissivity factor of all the liquids under study. The images of bentonite droplet evaporation are presented in Figure S1c (Supplementary Material). Next comes the fire-retardant solution. The difference in the evaporation times between bentonite and the fire-retardant ranges from 5 to 20% (decreasing with temperature growth). The fire retardant (Figure 1e) is a red-colored, opaque composition. Therefore, it also absorbs heat more actively (evaporates more rapidly) than the other compositions under study. Water, bischofite and OS-5 solutions, as well as the foaming agent emulsions, are optically transparent. Their $\varepsilon c_0 T_g^4$ is almost equal (until the moment when solid deposits start to form). Thus, at the initial heating and evaporation stages, the liquid evaporation will be conditioned by the density, heat transfer and latent heat of evaporation.

3.3. Experimental Curve Fitting

Table 3 summarizes the results of a mathematical description of the curves of complete evaporation times of fire extinguishing agent droplets versus the surface temperature and ambient temperature when using different heat supply mechanisms.

Table 3. Approximation coefficients.

Fire Extinguishing Agent	1	2	3	4	5	6	7	8	9	10	11	12	13
Conductive heating ($\tau = a_\alpha \cdot T^{b_\alpha}$)													
$a_\lambda \cdot 10^6$	2.54	3.63	3.75	4.38	3.25	3.40	4.46	4.93	3.72	4.02	4.01	2.63	2.48
b_λ	−2.4	−2.4	−2.4	−2.4	−2.4	−2.4	−2.4	−2.4	−2.4	−2.4	−2.4	−2.4	−2.4
R ²	0.99	0.99	0.99	0.98	0.99	0.99	1.00	0.99	0.99	0.99	0.99	0.99	0.98
Convective heating ($\tau = a_\alpha \cdot T^{b_\alpha}$)													
$a_\alpha \cdot 10^5$	0.84	0.91	1.06	0.97	0.93	0.84	0.95	1.00	1.04	0.76	0.75	0.85	0.97
b_α	−1.2	−1.2	−1.2	−1.2	−1.2	−1.2	−1.2	−1.2	−1.2	−1.2	−1.2	−1.2	−1.2
R ²	0.95	0.99	0.97	0.99	0.97	0.94	0.98	0.94	0.87	0.89	0.83	0.99	0.99
Radiant heating ($\tau = a_\varepsilon \cdot T^{b_\varepsilon}$)													
$a_\varepsilon \cdot 10^5$	6.93	8.22	9.23	7.78	6.25	5.72	19.92	7.76	7.17	8.24	7.55	7.88	7.77
b_ε	−1.6	−1.6	−1.6	−1.6	−1.6	−1.6	−1.6	−1.6	−1.6	−1.6	−1.6	−1.6	−1.6
R ²	0.99	0.99	0.99	0.99	0.98	0.98	0.99	0.99	0.99	0.98	0.99	0.98	0.99
Heating over an open flame ($\tau = a_f \cdot T^2 + b_f \cdot T + c_f$)													
a_f	7.2	3.2	3.1	4.9	2.7	1.7	4.0	2.8	4.8	2.8	2.2	3.2	3.2
b_f	−34.7	−20.6	−16.0	−21.9	−13.7	−5.0	−17.7	−12.1	−19.6	−11.5	−10.9	−13.1	−14.5
c_f	52.2	63.0	51.9	33.6	29.6	16.6	30.9	23.8	30.0	25.1	27.6	24.7	28.0
R ²	0.98	1.00	0.95	0.92	0.95	0.97	0.98	0.98	0.95	1.00	0.99	0.98	0.94

1—water; 2—flame retardant FR-Les (5% solution); 3—FR-Les (20% solution); 4—bentonite slurry (1%); 5—bentonite slurry (5%); 6—bischofite solution (5%); 7—bischofite solution (10%); 8—fire extinguishing agent OS-5 (5% solution); 9—fire extinguishing agent OS-5 (10% solution); 10—fire extinguishing agent OS-5 (15% solution); 11—foaming agent emulsion (1%); 12—foaming agent emulsion (5%); 13—fire retardant solution (5%).

It was established that the curves in the conductive, convective and radiant heating (in the muffle furnace) are similar and are described by a power function such as $\tau = a \cdot T^b$. It is noteworthy that a buffer vapor zone forms around droplets during evaporation in all

three cases of heat supply. This zone reduces the heat flow supplied to the droplet. As a result, a rise in the surface temperature and ambient temperature increases the vapor zone thickness due to the injection of a greater volume of vapor, while hardly changing the droplet temperature field. Therefore, during conductive, convective and radiant heating, the evaporation time first falls sharply and then, starting from a certain temperature, remains almost constant. When a droplet evaporates over an open flame, the $\tau = f(T)$ dependence is given by a second-degree polynomial.

Under identical evaporation conditions (thermal conductivity, convection and radiation), the power coefficient $b_{\lambda,\alpha,\varepsilon}$ takes the same value in the approximation for all the investigated liquids. It can be assumed that $b_{\lambda,\alpha,\varepsilon}$ depends only on the heat supply conditions. The coefficient $a_{\lambda,\alpha,\varepsilon}$ varies for different compositions. An assumption was made that $a_{\lambda,\alpha,\varepsilon}$ depends on the physical properties of a firefighting liquid. Unlike the curves in Figures 7–9, the ones in Figure 10 for the evaporation time of specialized fire extinguishing agent and water droplets are given by a second-degree polynomial: $\tau = a_f \cdot T^2 + b_f \cdot T + c_f$. The reason for that is that the temperature was at its maximum (~ 850 °C) at a distance of 2 cm from the burner wick. With an increase in the distance, the temperature falls, thus increasing the evaporation time. The trends and mathematical equations derived in this work allow predicting the characteristics of fire extinguishing agent evaporation at different temperatures and in different heat flows to be adapted to forest fire containment and suppression.

4. Conclusions

The characteristics of wettability (contact angles) and evaporation (evaporation time) suggest that a foaming agent and OS-5 with a concentration of more than 5% and 10% do not significantly improve fire suppression efficiency compared to water. A comparative analysis shows that the evaporation times of droplets of water, 5% fire retardant, FR-Les and bischofite solutions, as well as 1% bentonite slurry, differ only slightly. This finding is explained by the fact that the numerical values of the thermophysical properties of these liquids (density, heat capacity) and contact angles (thus, the droplet interaction area and the liquid–air interface) are very similar. The evaporation of liquids based on water and fire extinguishing agents (bentonite, bischofite, FR-Les and OS-5) leaves a solid residue (bentonite, salt crystals of MgCl_2 , ammonium polyphosphate and diammonium phosphate–carbamide).

The comparison of the evaporation times of specialized fire extinguishing agents under different heat supply conditions indicates that in radiant heating (in a muffle and above the burner) and convective heating of droplets, the longest evaporation time and the highest evaporation rate were typical of the 20% and 5% FR-Les solutions. In convective heating, the lowest evaporation time was recorded for the 10% OS-5 solution. In radiant heating, the lowest evaporation time was recorded for the 5% bentonite slurry. The differences in the evaporation time are attributed to the varying thermophysical properties of liquids. Therefore, in different heat supply schemes, dominant heat absorption mechanisms will differ.

The curves obtained for the evaporation time of specialized fire extinguishing agent droplets during conductive (on a solid surface), convective (in a wind tunnel) and radiant (in a muffle and over an open flame) heating were approximated by functions like $\tau = a \cdot T^b$ and $\tau = a_f \cdot T^2 + b_f \cdot T + c_f$. The obtained empirical coefficients are fundamental for the mathematical modeling of the processes under consideration. The established features of the effect of concentrations of specialized additives in water are of particular importance for practice. The values of limiting concentrations have been established, the excess of which will not lead to significant changes in the characteristics of the evaporation of droplets of fire extinguishing compositions; therefore, it is possible to prevent the over expenditure of specialized additives. For example, the use of OS-5 compositions and a foaming agent with concentrations above 10% and 1%, respectively, will not lead to qualitative changes during extinguishing.

Supplementary Materials: The following supporting information can be downloaded at: <https://www.mdpi.com/article/10.3390/f14020301/s1>, Figure S1: Typical images of the evaporation of specialized fire extinguishing agent droplets: (a) evaporation of FR-Les solution (20%) droplets when heated over an open flame at $h = 2$ cm (the initial droplet size is marked in red); (b) evaporation of OS-5 solution (10%) droplets during convective heating ($T = 500$ °C); (c) evaporation of bentonite slurry (10%) droplets during radiant heating in a muffle ($T = 400$ °C).

Author Contributions: A.Z.—writing—original draft preparation of manuscript; A.I.—writing—original draft; R.K.—conducting pilot studies; R.V.—planning and conducting experiments. All authors have read and agreed to the published version of the manuscript.

Funding: This research was funded by Russian Science Foundation, project No. 21-79-00030, <https://rscf.ru/project/21-79-00030/> (accessed on 1 February 2023).

Data Availability Statement: Not applicable.

Acknowledgments: This research was supported by the Russian Science Foundation (project No. 21-79-00030, <https://rscf.ru/project/21-79-00030/>). The authors would like to thank the staff of the Heat-Mass Transfer Laboratory of National Research Tomsk Polytechnic University (<http://hmtslab.tpu.ru> (accessed on 1 February 2023)) for assisting in the experimental research.

Conflicts of Interest: The authors declare no conflict of interest.

References

1. Lanotte, L.; Laux, D.; Charlot, B.; Abkarian, M. Role of red cells and plasma composition on blood sessile droplet evaporation. *Phys. Rev. E* **2017**, *96*, 053114. [[CrossRef](#)] [[PubMed](#)]
2. Park, J.; Lee, D.; Kim, W.; Horiike, S.; Nishimoto, T.; Se, H.L.; Ahn, C.H. Fully packed capillary electrochromatographic microchip with self-assembly colloidal silica beads. *Anal. Chem.* **2007**, *79*, 3214–3219. [[CrossRef](#)] [[PubMed](#)]
3. Kuznetsov, G.V.; Kralinova, S.S.; Voytkov, I.S.; Islamova, A.G. Rates of high-temperature evaporation of promising fire-extinguishing liquid droplets. *Appl. Sci.* **2019**, *9*, 5190. [[CrossRef](#)]
4. Borodulin, V.Y.; Letushko, V.N.; Nizovtsev, M.I.; Sterlyagov, A.N. The Experimental Study of Evaporation of Water–Alcohol Solution Droplets. *Colloid J.* **2019**, *81*, 219–225. [[CrossRef](#)]
5. Sobac, B.; Brutin, D. Thermocapillary instabilities in an evaporating drop deposited onto a heated substrate. *Phys. Fluids* **2012**, *24*, 032103. [[CrossRef](#)]
6. Caddock, B.D.; Hull, D. Influence of humidity on the cracking patterns formed during the drying of sol-gel drops. *J. Mater. Sci.* **2002**, *37*, 825–834. [[CrossRef](#)]
7. Shin, S.; Jacobi, I.; Stone, H.A. Bénard-Marangoni instability driven by moisture absorption. *Europhys. Lett.* **2016**, *113*, 24002. [[CrossRef](#)]
8. Xu, W.; Leeladhar, R.; Kang, Y.T.; Choi, C.-H. Evaporation Kinetics of Sessile Water Droplets on Micropillared Superhydrophobic Surfaces. *Langmuir* **2013**, *29*, 6032–6041. [[CrossRef](#)]
9. Koga, S.; Inasawa, S. Packing structures and formation of cracks in particulate films obtained by drying colloid–polymer suspensions. *Colloids Surf. A Physicochem. Eng. Asp.* **2019**, *563*, 95–101. [[CrossRef](#)]
10. Ryu, S.A.; Kim, J.Y.; Kim, S.Y.; Weon, B.M. Drying-mediated patterns in colloid-polymer suspensions. *Sci. Rep.* **2017**, *7*, 1079. [[CrossRef](#)]
11. Yamamura, M.; Ono, H.; Uchinomiya, T.; Mawatari, Y.; Kage, H. Multiple crack nucleation in drying nanoparticle-polymer coatings. *Colloids Surf. A Physicochem. Eng. Asp.* **2009**, *342*, 65–69. [[CrossRef](#)]
12. Harikrishnan, A.R.; Dhar, P. Optical thermogeneration induced enhanced evaporation kinetics in pendant nanofluid droplets. *Int. J. Heat Mass Transf.* **2018**, *118*, 1169–1179. [[CrossRef](#)]
13. Yu, M.; Le Floch-Fouéré, C.; Pauchard, L.; Boissel, F.; Fu, N.; Chen, X.D.; Saint-Jalmes, A.; Jeantet, R.; Lanotte, L. Skin layer stratification in drying droplets of dairy colloids. *Colloids Surf. A Physicochem. Eng. Asp.* **2021**, *620*, 126560. [[CrossRef](#)]
14. Hampton, M.A.; Nguyen, T.A.H.; Nguyen, A.V.; Xu, Z.P.; Huang, L.; Rudolph, V. Influence of surface orientation on the organization of nanoparticles in drying nanofluid droplets. *J. Colloid Interface Sci.* **2012**, *377*, 456–462. [[CrossRef](#)]
15. Deegan, R.D.; Bakajin, O.; Dupont, T.F.; Huber, G.; Nagel, S.R.; Witten, T.A. Capillary flow as the cause of ring stains from dried liquid drops. *Nature* **1997**, *389*, 827–829. [[CrossRef](#)]
16. Li, W.; Ji, W.; Sun, H.; Lan, D.; Wang, Y. Pattern Formation in Drying Sessile and Pendant Droplet: Interactions of Gravity Settling, Interface Shrinkage, and Capillary Flow. *Langmuir* **2019**, *35*, 113–119. [[CrossRef](#)]
17. Daïf, A.; Bouaziz, M.; Chesneau, X.; Ali Chérif, A. Comparison of multicomponent fuel droplet vaporization experiments in forced convection with the Sirignano model. *Exp. Therm. Fluid Sci.* **1998**, *18*, 282–290. [[CrossRef](#)]
18. Han, K.; Yang, B.; Zhao, C.; Fu, G.; Ma, X.; Song, G. Experimental study on evaporation characteristics of ethanol–diesel blend fuel droplet. *Exp. Therm. Fluid Sci.* **2016**, *70*, 381–388. [[CrossRef](#)]

19. Hallett, W.L.H.; Beauchamp-Kiss, S. Evaporation of single droplets of ethanol–fuel oil mixtures. *Fuel* **2010**, *89*, 2496–2504. [[CrossRef](#)]
20. Shringi, D.; Dwyer, H.A.; Shaw, B.D. Influences of support fibers on vaporizing fuel droplets. *Comput. Fluids* **2013**, *77*, 66–75. [[CrossRef](#)]
21. Shih, A.T.; Megaridis, C.M. Suspended droplet evaporation modeling in a laminar convective environment. *Combust. Flame* **1995**, *102*, 256–270. [[CrossRef](#)]
22. Korobeinichev, O.P.; Shmakov, A.G.; Chernov, A.A.; Bol'shova, T.A.; Shvartsberg, V.M.; Kutsenogii, K.P.; Makarov, V.I. Fire suppression by aerosols of aqueous solutions of salts. *Combust. Explos. Shock Waves* **2010**, *46*, 16–20. [[CrossRef](#)]
23. Mykhalichko, B.; Lavrenyuk, H.; Mykhalichko, O. New water-based fire extinguishant: Elaboration, bench-scale tests, and flame extinguishment efficiency determination by cupric chloride aqueous solutions. *Fire Saf. J.* **2019**, *105*, 188–195. [[CrossRef](#)]
24. Rakowska, J.; Szczygieł, R.; Kwiatkowski, M.; Porycka, B.; Radwan, K.; Prochaska, K. Application Tests of New Wetting Compositions for Wildland Firefighting. *Fire Technol.* **2017**, *53*, 1379–1398. [[CrossRef](#)]
25. Rakowska, J.; Prochaska, K.; Twardochleb, B.B.; Rojewska, M.; Porycka, B.B.; Jazzkiewicz, A. Selection of surfactants as main components of ecological wetting agent for effective extinguishing of forest and peat-bog fires. *Chem. Pap.* **2014**, *68*, 823–833. [[CrossRef](#)]
26. Appah, S.; Zhou, H.; Wang, P.; Ou, M.; Jia, W. Charged monosized droplet behaviour and wetting ability on hydrophobic leaf surfaces depending on surfactant-pesticide concentrate formulation. *J. Electrostat.* **2019**, *100*, 103356. [[CrossRef](#)]
27. Glenn, G.M.; Bingol, G.; Chiou, B.-S.; Klamczynski, A.P.; Pan, Z. Sodium bentonite-based coatings containing starch for protecting structures in wildfire emergency situations. *Fire Saf. J.* **2012**, *51*, 85–92. [[CrossRef](#)]
28. Brahmia, F.Z.; Alpár, T.; Horváth, P.G.; Csiha, C. Comparative analysis of wettability with fire retardants of Poplar (*Populus cv. euramericana I214*) and Scots pine (*Pinus sylvestris*). *Surf. Interfaces* **2020**, *18*, 100405. [[CrossRef](#)]
29. Jenkins, M.S.; Bedward, M.; Price, O.; Bradstock, R.A. Modelling bushfire fuel hazard using biophysical parameters. *Forests* **2020**, *11*, 925. [[CrossRef](#)]
30. Robinne, F.-N.; Miller, C.; Parisien, M.-A.; Emelko, M.B.; Bladon, K.D.; Silins, U.; Flannigan, M. A global index for mapping the exposure of water resources to wildfire. *Forests* **2016**, *7*, 22. [[CrossRef](#)]
31. Islamova, A.; Kropotova, S.; Tkachenko, P.; Voitkov, I.; Kuznetsov, G. Transformation of Initially Unatomized Fire-Extinguishing Liquid Arrays at Free Fall from Different Heights. *At. Sprays* **2021**, *31*, 71–91. [[CrossRef](#)]
32. Alsammak, I.L.H.; Mahmoud, M.A.; Aris, H.; Alkilabi, M.; Mahdi, M.N. The Use of Swarms of Unmanned Aerial Vehicles in Mitigating Area Coverage Challenges of Forest-Fire-Extinguishing Activities: A Systematic Literature Review. *Forests* **2022**, *13*, 811. [[CrossRef](#)]
33. Kuznetsov, G.; Zhdanova, A.; Voitkov, I.; Strizhak, P. Disintegration of Free-falling Liquid Droplets, Jets, and Arrays in Air. *Microgravity Sci. Technol.* **2022**, *34*, 12. [[CrossRef](#)]
34. Rodríguez-Veiga, J.; Ginzo-Villamayor, M.J.; Casas-Méndez, B. An integer linear programming model to select and temporally allocate resources for fighting forest fires. *Forests* **2018**, *9*, 583. [[CrossRef](#)]
35. GOST R 50588-2012; Foaming Agents for Fire Extinguishing. General Technical Requirements and Test Methods. Standardinform: Moscow, Russia, 2012.
36. GOST 16363-98; Fire Protective Means for Wood. Methods for Determination of Fire Protective Properties. Standardinform: Moscow, Russia, 1998.
37. GOST 7759-73; Technical Magnesium Chloride (Bishofit). Specifications. Standardinform: Moscow, Russia, 1991.
38. Shadrina, E.M.; Volkova, G.V. *Determination of Thermophysical Properties of Gases, Liquids and Aqueous Solutions of Substances*; Ivanovo University of Chemical Technology: Ivanovo, Russia, 2009.
39. Kuznetsov, G.V.; Islamova, A.G.; Orlova, E.G.; Strizhak, P.A.; Feoktistov, D.V. Physicochemical features of the effect of special water-based fire retardants on forest materials. *Fire Saf. J.* **2021**, *123*, 103371. [[CrossRef](#)]
40. Antonov, D.V.; Fedorenko, R.M.; Strizhak, P.A.; Nissar, Z.; Sazhin, S.S. Puffing/micro-explosion in composite fuel/water droplets heated in flames. *Combust. Flame* **2021**, *233*, 111599. [[CrossRef](#)]
41. Soboleva, O.A. Enrichment and Leaning of the Area near the Line of Wetting by Surfactants, Msu Vestnik. Series 2. *Chemistry* **2003**, *44*, 337–341.
42. Volkov, R.S.S.; Strizhak, P.A.A. Research of temperature fields and convection velocities in evaporating water droplets using Planar Laser-Induced Fluorescence and Particle Image Velocimetry. *Exp. Therm. Fluid Sci.* **2018**, *97*, 392–407. [[CrossRef](#)]

Disclaimer/Publisher's Note: The statements, opinions and data contained in all publications are solely those of the individual author(s) and contributor(s) and not of MDPI and/or the editor(s). MDPI and/or the editor(s) disclaim responsibility for any injury to people or property resulting from any ideas, methods, instructions or products referred to in the content.